$$E_{22} = \cos(T - \theta_1)\cos\phi_1 \sin(\phi_1 - \phi_2) - \cos T \sin\phi_1 \cos(\phi_1 - \phi_2) \equiv C\cos T + D \sin T \tag{1}$$

where

$$T = \omega t - \delta_1 - \delta_2 - \tau \tag{2}$$

and C, D, E, F are defined by these equations.

The resultant of these two components sweeps out an ellipse as T increases, and the cross polarization is simply the ratio of the semi-major and semi-minor axes. These may be found by rotating the E_{21}, $E_{22}(X, Y)$ axes by a positive angle α to a new pair of axes (x, y). α is chosen so that the cross product xy of the ellipse equation in (x, y) coordinates vanishes.

This criterion is found to be

$$\alpha = \frac{1}{2}\tan^{-1}\left\{\frac{2(CE + DF)}{E^2 + F^2 - C^2 - D^2}\right\} \tag{3}$$

and the ellipse equation is then

$$\frac{x^2}{R^2} + \frac{y^2}{S^2} = 1 \tag{4}$$

where

$$R^2 = \left[\frac{(CF - DE)^2}{(C^2 + D^2)\cos^2\alpha - (CE + DF)\sin 2\alpha + (E^2 + F^2)\sin^2\alpha}\right] \tag{5}$$

and

$$S^2 = \left[\frac{(CF - DE)^2}{(C^2 + D^2)\sin^2\alpha + (CE + DF)\sin 2\alpha + (E^2 + F^2)\cos^2\alpha}\right].$$

The cross polarization is then

$$\text{C.P.}_{\text{db}} = -10\left|\log\left(\frac{R^2}{S^2}\right)\right|. \tag{6}$$

The necessary functions of C, D, E, F are found to be

$$\begin{aligned} C^2 + D^2 &= \cos^2\phi_1 \cdot \sin^2(\phi_1 - \phi_2) + \sin^2\phi_1 \cdot \cos^2(\phi_1 - \phi_2) - \tfrac{1}{2}\cdot\sin 2\phi_1 \cdot \sin(2\phi_1 - 2\phi_2)\cdot\cos\theta_1 \\ E^2 + F^2 &= \cos^2\phi_1 \cdot \cos^2(\phi_1 - \phi_2) + \sin^2\phi_1 \cdot \sin^2(\phi_1 - \phi_2) + \tfrac{1}{2}\cdot\sin 2\phi_1 \cdot \sin(2\phi_1 - 2\phi_2)\cdot\cos\theta_1 \\ CE + DF &= \tfrac{1}{2}\cdot\cos 2\phi_1 \cdot \sin(2\phi_1 - 2\phi_2)\cdot\cos\theta_2 + \tfrac{1}{2}\sin^2(\phi_1 - \phi_2)\cdot\sin 2\phi_1 \cdot\cos(\theta_1 - \theta_2) - \tfrac{1}{2}\cos^2(\phi_1 - \phi_2)\cdot\sin 2\phi_1 \cdot \cos(\theta_1 + \theta_2). \end{aligned} \tag{7}$$

Figures 2 to 7 give computed results for the worst cross polarization (ϕ_2 was varied in steps and worst value chosen) for various reasonable combinations of $\phi_1, \theta_1, \theta_2$. The expression for cross polarization may be greatly simplified by assuming differential phase shifts close to $\pi/2$ and ϕ_1 close to $\pi/4$, if desired.

ACKNOWLEDGMENT

The author is indebted to W. Lavrench for a discussion of this work.

R. W. BREITHAUPT
Radio and Elect. Engrg. Div.
National Research Council
Ottawa, Canada

Solid-State Plasma Controlled Nonreciprocal Microwave Device

Various types of nonreciprocal microwave devices have been developed through the use of the tensor permeability of magnetic materials such as ferrites.[1] In a solid-state plasma such as a semiconductor, the conductivity becomes a tensor quantity under a dc magnetic field. Toda[2] developed an isolator using a solid-state plasma under a transverse magnetic field and obtained the isolation ratio of about 10 dB. Recently, we have reported the result of the experimental observation of the microwave Faraday effect in a solid-state plasma waveguide under a longitudinal magnetic field.[3] It was found that a large amount of rotation of the plane of polarization with very small attenuation of power can be obtained in a solid-state plasma under a relatively high magnetic field. In this paper, an experimental nonreciprocal microwave device which makes use of the Faraday rotation in a solid-state plasma is presented.

The experimental microwave device consists of two rectangular waveguides, two resistance vanes, and a solid-state plasma Faraday rotator as shown in Fig. 1. The Faraday rotator consists of a circular waveguide (7 mm ID) in which a disk (7 mm $D \times 1$ mm T) of an n-type InSb single crystal ($n_e = 10^{14}/\text{cm}^3$, $\mu_e = 70\,000$ cm^2/V.s, $\rho = 0.1$ Ω-cm, at 77°K) and two quarter-wavelength impedance transformers ($\epsilon_r = 4$) are mounted as shown in Fig. 1. The impedance transformers are placed at both sides of the InSb disk to minimize the wave reflections from the surfaces of the InSb disk. The resistance vanes are mounted in such a way as to attenuate the components of electric field which are parallel to the broad walls of the rectangular guides. The transitions between the rectangular and circular guides are made smooth by means of tapered transitions. The two rectangular guides are rotated 45° with respect to each other.

A linearly polarized wave, after passing through the solid-state plasma, becomes an elliptically polarized wave in which the major axis of polarization is rotated through an angle with respect to the plane of polarization of the incident wave. The angle of the Faraday rotation Θ and the ellipticity of polarization $\mathcal{E}$ vary as a function of the magnetic field B_0. (Details of the principle of the Faraday effect in a solid-state plasma can be found elsewhere.[3]) The direction of the rotation depends on the direction of propagation with respect to the direction of the magnetic field. For example, if the magnetic field is applied in the direction as shown in Fig. 1, the wave propagating from left to right experiences clockwise rotation due to the Faraday rotator, while the wave propagating in the opposite direction experiences counterclockwise rotation.

Let T be the transmission coefficient of the Faraday rotator. Then the insertion loss of the device for the transmission from left to right will be

$$L_1 = -10\log\left[T^2\{\cos^2(\Theta - 45°) + \mathcal{E}^2\sin^2(\Theta - 45°)\}\right]$$

and for the transmission in the opposite direction, we get

$$L_2 = -10\log\left[T^2\{\cos^2(\Theta + 45°) + \mathcal{E}^2\sin^2(\Theta + 45°)\}\right]$$

Thus we can achieve nonreciprocal transmission through this device. By varying the magnetic field, we can control Θ and in turn we can control L_1 and L_2. When $\Theta = 45° + n \times 180°$ where n is an integer, the difference between L_1 and L_2 will be maximized. By reversing the direction of the magnetic field, we can switch L_1 and L_2 from maximum to minimum or vice versa. Thus the experimental device can be used as an attenuator, isolator, or switch.

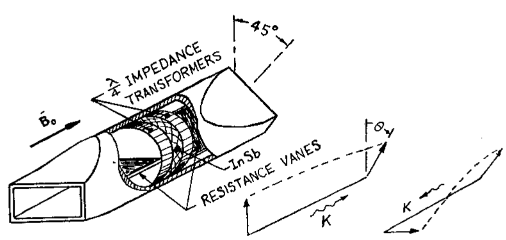

Fig. 1. An experimental solid-state plasma controlled nonreciprocal microwave device.

The characteristics of the experimental device were measured under various magnetic fields using the set-up as shown in Fig. 2. The device was placed between a pair of poles of a magnet and immersed in liquid nitrogen to cool the InSb crystal so that μ_e and ρ were increased. The klystron was tuned to $f = 35.95$ GHz. Figure 3 shows the measured nonreciprocal transmission characteristics. The points where $B_0 = 1.1$, 2.8, and 8.5 kg correspond to $\Theta = 225°$, 135°, and 45°, respectively. In particular, at $B_0 = 8.5$ kg, an excel-

Manuscript received August 23, 1966. This work is partly based on dissertation research by the author and is supported in part by a NASA research grant.

[1] See, for example, C. L. Hogan, "The elements of nonreciprocal microwave device," *Proc. IRE*, vol. 44, pp. 1345–1368, October 1956; and B. Lax and K. J. Button, *Microwave Ferrites and Ferrimagnetics*. New York: McGraw-Hill, 1962, ch. 12.

[2] M. Toda, "A new isolator using a solid-state plasma waveguide," *IEEE Trans. on Microwave Theory and Techniques (Correspondence)*, vol. MTT-12, pp. 126–127, January 1965.

[3] H. J. Kuno and W. D. Hershberger, "Observation of microwave Faraday rotation in a solid-state plasma," *Proc. IEEE (Letters)*, vol. 54, pp. 978–979, July 1966.

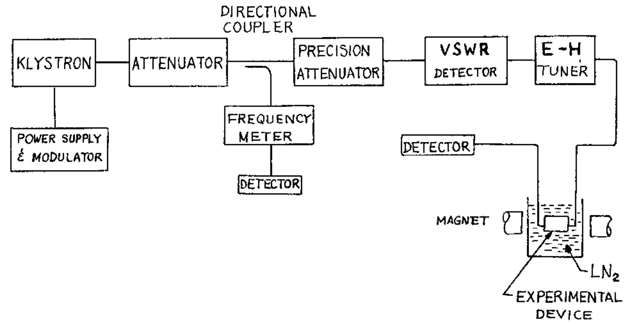

Fig. 2. Experimental set-up for the measurement of characteristics of the experimental microwave device.

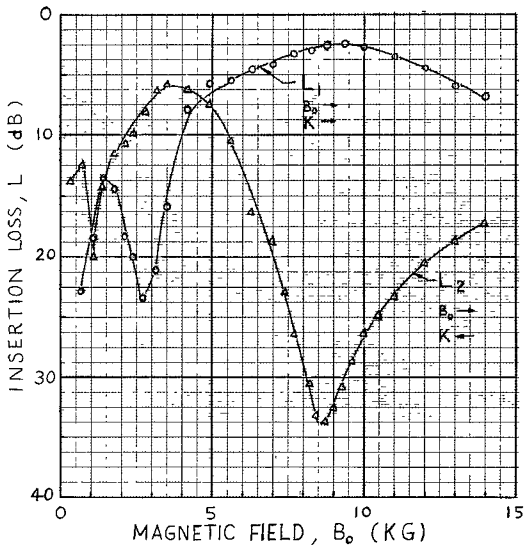

Fig. 3. Measured nonreciprocal transmission characteristics of the experimental microwave device as a function of magnetic field.

lent isolation ratio was achieved. The measured isolation ratio at this point was 30 dB, i.e., the ratio of 1000 to 1 in power between L_1 and L_2.

We have thus demonstrated an example of possible microwave device applications of the Faraday effect in solid-state plasmas. The theoretical upper limit of frequency of the solid-state plasma device will appear at the cyclotron resonant frequency which is higher than 1000 GHz in the present case. Although the present experiment was conducted at a K_a-band frequency, the technique can, therefore, be extended to higher frequency regions such as submillimeter waves.

H. J. KUNO
W. D. HERSHBERGER
Dept. of Engrg.
University of California
Los Angeles, Calif.

Further Generalization of Waveguide Theorems

In a recent paper by Laxpati and Mittra [1], the bidirectional waveguide theorems [2], [3] were extended to both periodic and open waveguide structures. In the original derivation of the theorems [2], [3] an artifice was employed in which Poynting's theorem was applied to a standing complex wave set up in the general bidirectional waveguide by a shorting plane. The point was well taken in the recent paper [1] that a short-circuit termination is not necessary and that the same results may be derived in just as straightforward a manner by considering a termination of arbitrary, non-zero reflection coefficient which also sets up a complex standing wave. The important features of the power and pseudo-energy relations result from the cross terms arising in the complex standing wave and are lost if only a traveling-wave without a reflection is operated on by Poynting's theorem.

In this correspondence we wish to point out that the bidirectional-waveguide theorems may be derived even without the artifice of an imperfect termination. Only the relations for a single wave in an infinite or matched waveguide need be considered [4]. Furthermore, the same basic theorems may be extended to apply to *nonbidirectional* waveguides as well [4]. Also, the constitutive relations characterizing the medium filling the waveguide can be generalized to include the Tellegen medium for which the relations apply [5]

$$\overline{D} = \bar{\bar{\epsilon}}\cdot\overline{E} + \bar{\bar{\gamma}}\cdot\overline{H} \tag{1}$$

$$\overline{B} = \bar{\bar{\mu}}\cdot\overline{H} + \bar{\bar{\xi}}\cdot\overline{E}. \tag{2}$$

The Tellegen medium of course reduces to the more ordinary anisotropic medium when $\bar{\bar{\xi}}$ and $\bar{\bar{\gamma}}$ vanish. In this correspondence we shall confine our attention to the lossless, passive systems. Thus for the Tellegen medium, the following relations must apply [5]

$$\bar{\bar{\epsilon}} = \bar{\bar{\epsilon}}^{+} \qquad \bar{\bar{\mu}} = \bar{\bar{\mu}}^{+} \qquad \bar{\bar{\gamma}} = \bar{\bar{\xi}}^{+} \tag{3}$$

where the superscript (+) has been used to denote the conjugate transpose of a tensor.

For a waveguide containing the general Tellegen medium, Maxwell's equations may be separated into transverse and longitudinal components for a single waveguide mode:

$$\nabla_T E_z + \Gamma \overline{E}_T = -j\omega \bar{i}_z \times \overline{B}_T \tag{4}$$

$$\nabla_T H_z + \Gamma \overline{H}_T = j\omega \bar{i}_z \times \overline{D}_T \tag{5}$$

$$\bar{i}_z \cdot \nabla_T \times \overline{E}_T = -j\omega B_z \tag{6}$$

$$\bar{i}_z \cdot \nabla_T \times \overline{H}_T = j\omega D_z \tag{7}$$

where Γ in general is the complex propagation constant for the mode. The relations leading to the waveguide theorems are formed by cross multiplying (4) by $\overline{H}_T^*$ and then dot multiplying by the unit vector $\bar{i}_z$. The result is

$$\begin{aligned}\Gamma(\overline{E}_T \times \overline{H}_T^*)\cdot\bar{i}_z &= j\omega\overline{H}_T^*\cdot\overline{B}_T - j\omega E_z D_z^* \\ &\quad - \bar{i}_z\cdot\nabla_T\times(E_z\overline{H}_T^*)\end{aligned} \tag{8}$$

where (7) has also been used. In a similar manner, we have from (5) and (6)

$$\begin{aligned}\Gamma^*(\overline{E}_T \times \overline{H}_T^*)\cdot\bar{i}_z &= -j\omega\overline{E}_T\cdot\overline{D}_T^* + j\omega H_z^* B_z \\ &\quad + \bar{i}_z\cdot\nabla_T\times(H_z^*\overline{E}_T).\end{aligned} \tag{9}$$

When (8) and (9) are integrated over the cross section of the waveguide, we obtain the relations[1]

$$(\alpha + j\beta)(P + jQ) = j2\omega(U_{mT} - U_{ez}) \tag{10}$$

$$(\alpha - j\beta)(P + jQ) = j2\omega(U_{mz} - U_{eT}). \tag{11}$$

The quantities appearing in these equations have the definitions of

a) complex power

$$P + jQ = \frac{1}{2}\int \overline{E}_T \times \overline{H}_T^*\cdot\bar{i}_z da, \tag{12}$$

b) transverse magnetic pseudo energy

$$U_{mT} = \frac{1}{4}\int \overline{H}_T^*\cdot\overline{B}_T da, \tag{13}$$

c) transverse electric pseudo energy

$$U_{eT} = \frac{1}{4}\int \overline{E}_T\cdot\overline{D}_T^* da, \tag{14}$$

d) longitudinal magnetic pseudo energy

$$U_{mz} = \frac{1}{4}\int H_z^* B_z da, \tag{15}$$

e) longitudinal electric pseudo energy

$$U_{ez} = \frac{1}{4}\int E_z D_z^* da. \tag{16}$$

An important feature to note at this point is that the pseudo energies defined here are in general complex quantities except for the special case of bidirectional waveguides. For bidirectional waveguides, they are all pure real since $\overline{B}_T$ and $\overline{D}_T$ involve only $\overline{H}_T$ and $\overline{E}_T$, respectively, and B_z and D_z involve only H_z and E_z, respectively.

Manuscript received July 22, 1966. This work was supported in part by Joint Services Electronics Program Contract DA-36-039-AMC-03200(E) and National Science Foundation Grant GK-614.

[1] The terms involving the transverse curls vanish by applying Stokes' Theorem and the boundary conditions at perfect electric and/or magnetic walls.